Applied Mathematics & Information Sciences
An International Journal

http://dx.doi.org/10.12785/amis/081L28

Knowledge-based Principal Component Analysis for Image Fusion

Jie-Lun Chiang∗

Department of Soil and Water Conservation, National Pingtung University of Science and Technology, Pingtung County, 912, Taiwan

Received: 4 May. 2013, Revised: 29 Aug. 2013, Accepted: 30 Aug. 2013
Published online: 1 Apr. 2014

Abstract: The purpose of image fusion is to integrate images with different resolution or from different sources in order to increase information and reinforce identification and reliability in remote sensing application. The principal component analysis (PCA) approach is a commonly used method for satellite image fusing. In the PCA fusion process, the first principal component (PC1) image is replaced with a high resolution image (e.g., a Panchromatic (PAN) image of the SPOT4 satellite). When the histograms of PC1 and PAN images are more similar, less spectral information is lost in the replacement process.
In this study, a knowledge-based principal component analysis (KBPCA) fusion is developed to improve the fusing results of PCA approach. Before the replacement of PAN image, a prior landcover classification was done to gain the knowledge of the landcover of study area. Principal component transform was then conducted on the individual data set of each landcover class. Since the spectrum variation of each landcover class is smaller than that of the entire image, such pre-classification makes the PC1 of each class, have less spectrum variation, compared to the PC1 of the entire image. Landcover information derived from pre-classification is used as additional information to limit spectrum variation in each class for image fusion during the principal component transform. As a result of fusion, a multi-spectrum high resolution new image can be produced by fusing multispectral and PAN images of SPOT4. The images fused by the KBPCA method are of quality superior to those fused by the PCA method in terms of visual and statistical assessments.

Keywords: Merge, pan-sharpening, satellite imagery, image resolution

1 Introduction

Image fusion techniques have been developed for many years. It's been widely applied in various fields, such as military [1,2,3,4], medicine [5,6], chemistry [7], agriculture [8,9,10], robotics [11], environmental science [12,13,14,15,16], Bioinformatics [17,18], etc. The purpose of image fusion is to integrate images with different resolutions or even images from different sensors, such that identifiability and reliability of images are increased. The fusion of multispectral (MS) and panchromatic images is a very useful technique for remote sensing applications.

According to transformation domains, image fusion methods can be roughly classified into two types [19]: (1) spectral domain methods (e.g., PCA [20], HIS [21], etc.), and (2) special domain methods (e. g. high pass filter, linear combination transformation [20], etc.

The PCA technique [22,23,24,25,26,27,28] has been widely applied in image fusions of various fields due to its good performance. However, some information may get lost during the replacement process of PCA fusion. In this study, a knowledge-based principal component analysis (KBPCA) fusion is developed to improve the fusing results of the PCA approach.

2 Methodology

2.1 PCA Fusion

The principal component analysis (PCA) was previously well applied (first developed) for multivariate data reduction and interpretation in the field of statistics. In fact PCA was first developed for a linear transformation based on linear algebra. Eq. (1) shows the relationship between eigenvalues and eigenvectors of matrix A, where A is a $n\times n$ matrix, λ is an eigenvalue of matrix A, X is an eigenvector of matrix A, For $n = 3$, it can be expressed by Eq. (2)

$$(A-\lambda I)X = 0 \tag{1}$$

∗ Corresponding author e-mail: jlchiang@mail.npust.edu.tw

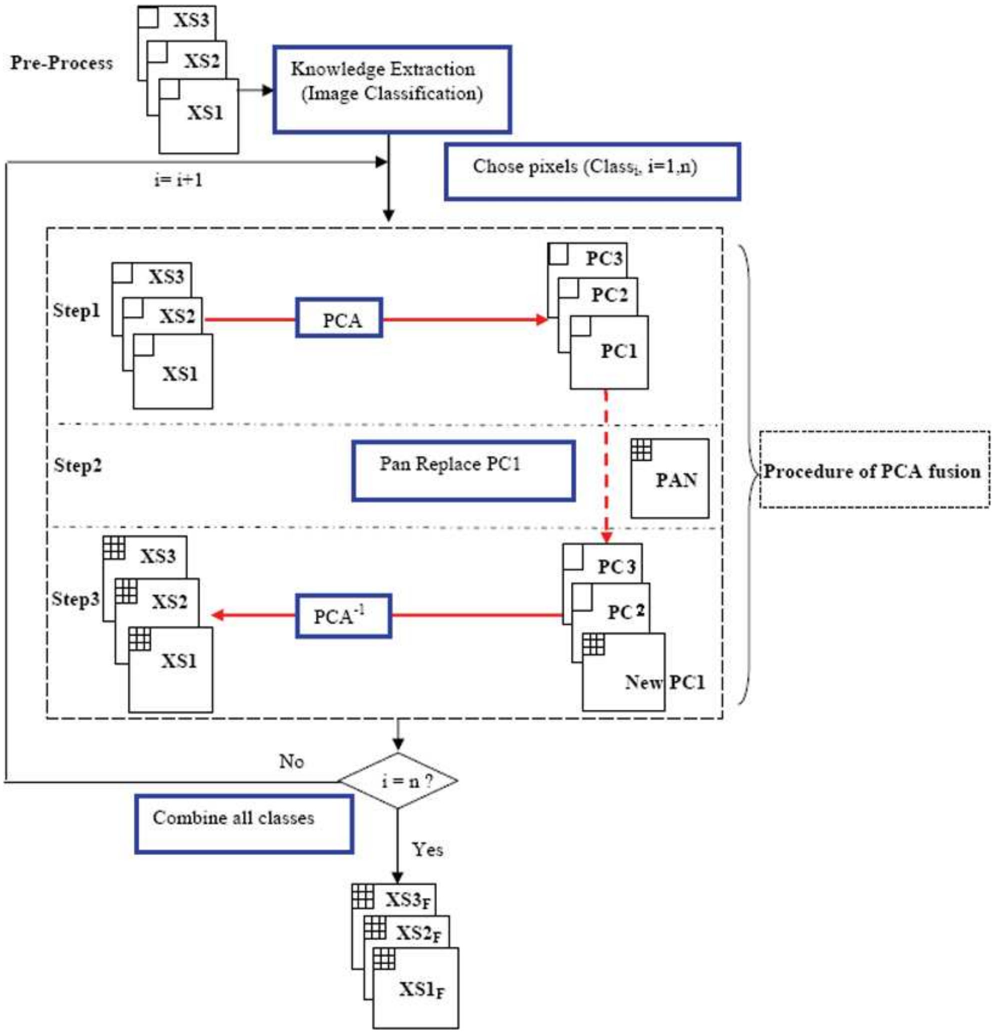

Fig. 1: Flow chart of KBPCA fusion.

$$\left(\begin{bmatrix} a_{11} & a_{12} & a_{13} \\ a_{21} & a_{22} & a_{23} \\ a_{31} & a_{32} & a_{33} \end{bmatrix} - \lambda \begin{bmatrix} 1 & 0 & 0 \\ 0 & 1 & 0 \\ 0 & 0 & 1 \end{bmatrix}\right) \cdot \begin{bmatrix} x_1 \\ x_2 \\ x_3 \end{bmatrix} = 0 \quad (2)$$

Through linear algebra, PCA can transform a dataset into a new coordinate system with orthogonal basis. In this paper, we consider the SPOT images XS1, XS2, XS3 as three random variables which have a 3×3 covariance matrix $\sum$. The eigenvalues $(\lambda 1, \lambda 2, \lambda 3)$ and eigenvectors (e1, e2, e3) can be determined, with e1, e2 and e3 linearly independent and pairwise orthogonal (i.e., their inner product equal zero $e_1 \cdot e_2 = 0$, $e_1 \cdot e_3 = 0$, $e_2 \cdot e_3 = 0$). Then, the first, second and third principal components (PC1, PC2, and PC3) can be determined as follows:

$$PC_1 = e_1' XS \quad (3)$$

$$PC_2 = e_2' XS \quad (4)$$

$$PC_3 = e_3' XS \quad (5)$$

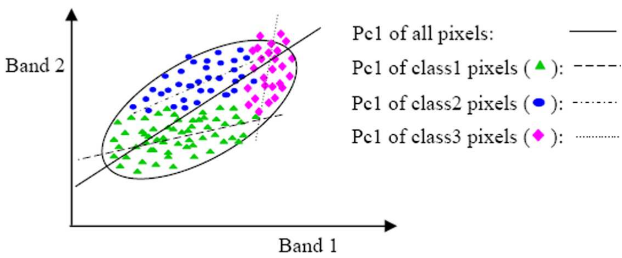

Fig. 2: PC1 of individual class and entire image.

Where $XS = \begin{bmatrix} xs_1 \\ xs_2 \\ xs_3 \end{bmatrix}$.

After rotating to the PC space (with the new axes, PC1, PC2 and PC3), we can determine the percentage of total variance explained by the n^{th} principal component as $\lambda_n / \Sigma \lambda_k$ with $1 \leqslant n, k \leqslant 3$. The procedure of PCA image

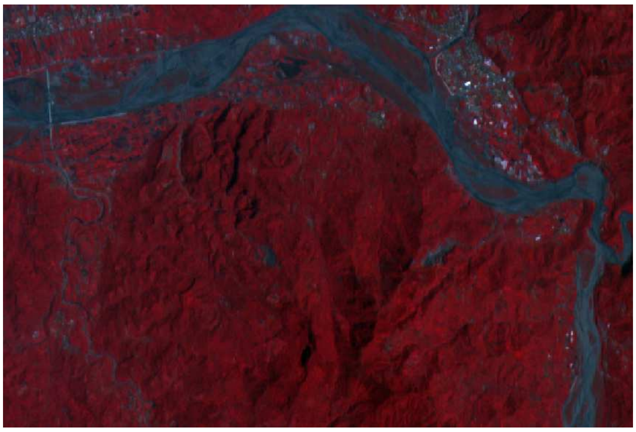

(a) Multispectral SPOT forces color image (XS1, XS2, XS3) (20m)

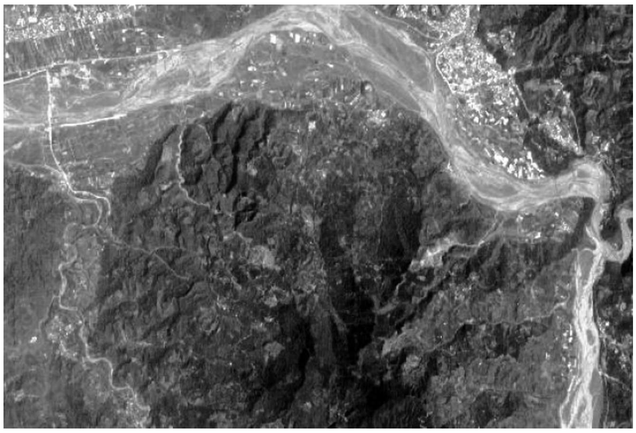

(b) Panchromatic SPOT image (10m)

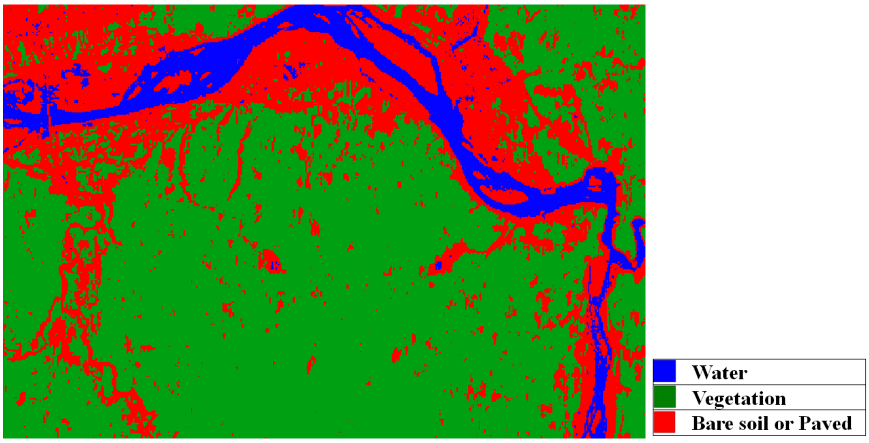

(c) Results of landcover classification

Fig. 3: SPOT images and landcover map of study area

fusion is shown in the central part of Fig. 1. Three-band multispectral images of SPOT (XS1, XS2 and XS3) are used as input to the principal component analysis procedure. After the multispectral images are transformed to the PC space, principal components PC1, PC2 and PC3 are determined, and then the PAN image is used to replace PC1. Finally, the new PC1 and the original PC2 and PC3 are retransformed back into the original space, and the fused multispectral images can be produced.

2.2 Knowledge-Based PCA

The proposed knowledge-based PCA is based on the ordinary PCA fusion approach. The intuition behind our approach is that a pre-processing step using image classification may offer us useful landcover information for the geological locations under study. From this landcover knowledge, image pixels can be separated into K (the number of categories) groups. In this paper we extract landcover information via a maxima likelihood classifier. After pre-classification, PCA was done in pixels of each individual class. The principal components (PC1, PC2, and PC3) can be determined via Eq. (6)–(8).

$$\text{If } XS \in Class1, \begin{bmatrix} PC_{1,c1} \\ PC_{2,c1} \\ PC_{3,c1} \end{bmatrix} = \begin{bmatrix} e'_{1,c1}XS \\ e'_{2,c1}XS \\ e'_{3,c1}XS \end{bmatrix} \tag{6}$$

$$\text{If } XS_i \in Class2, \begin{bmatrix} PC_{1,c2} \\ PC_{2,c2} \\ PC_{3,c2} \end{bmatrix} = \begin{bmatrix} e'_{1,c2}XS \\ e'_{2,c2}XS \\ e'_{3,c2}XS \end{bmatrix} \tag{7}$$

$$\vdots$$

$$\text{If } XS_i \in Classn, \begin{bmatrix} PC_{1,cn} \\ PC_{2,cn} \\ PC_{3,cn} \end{bmatrix} = \begin{bmatrix} e'_{1,cn}XS \\ e'_{2,cn}XS \\ e'_{3,cn}XS \end{bmatrix} \tag{8}$$

Then pixels of each landcover class were fused by PCA approach. Finally, the fused results can be obtained by combining all the classes as shown in Fig. 1. The reason why a pre-classification is beneficial in our

Table 1: Confusion matrix of maxima likelihood classification, p.s.: Kappa = 97.68%

Referenced / Classified	Water	Vegetation	Bare soil/Paved	Over all	User's Accuracy
Water	870	0	18	888	97.97
Vegetation	0	1810	0	1810	100.00
Bare soil/Paved	24	0	442	466	94.85
Over all	894	1810	460	3164	
Producer's Accuracy	97.32	100.00	97.68	Over all Accuracy %	98.67

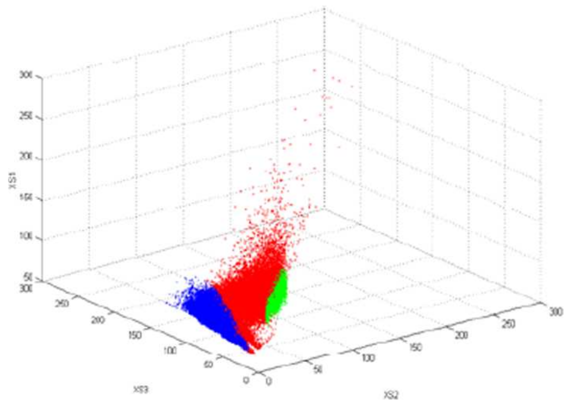

(a) Original space

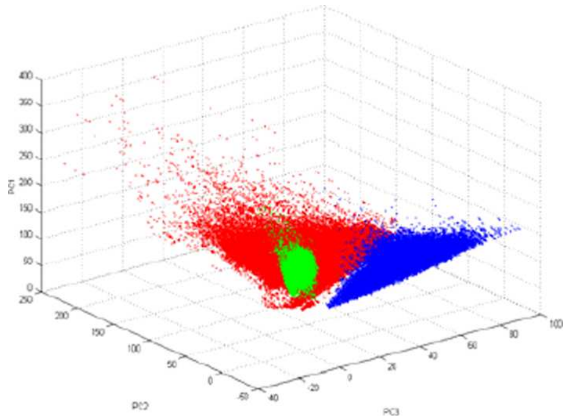

(b) PC space

Fig. 4: Scatterplots in original space and PC space

KBPCA process was shown as Fig. 2, where three kinds of dots distributed in a two dimensional feature space correspond to three landcover classes. As can be seen, the variation of each landcover class is smaller than that of the entire image in XS1, XS2, XS3 and PC1. Since the spectrum variation of each landcover class is smaller than that of the entire image, such pre-classification makes the PC1 of each class have less spectrum variation, compared to the PC1 of the entire image. Principal component transform is then conducted on the individual data set of each landcover class. Consequently the spectral information loss during PC1 replacement can be reduced.

3 Case study

3.1 Materials

An area of approximately 292 km^2 in Central Taiwan is selected for this study (Fig. 3). The image size is 702×1040. The study area includes a small township at the northeastern corner, a major river, with several small branches, flowing westward along the northern edge of the area, and nearby the mountainous area. Three major landcover classes (water, bare soil and paved area, vegetation) are identified in this study. Multispectral SPOT satellite images acquired on September 21, 2000 are used for the pre-classification and image fusion. The false color multispectral SPOT image is shown in Fig. 3(a). A total number of 3164 pixels (894 pixels for water, 1810 pixels for vegetation, and 460 pixels for bare soil/paved area) of this image is selected as training samples (which are selected based on field investigation and a 1/5,000-scale aerial photo of Nov. 18, 1999) for our landcover pre-classification. Three bands of multispectral data (XS1 (green) 0.5–0.59 μm, XS2 (red) 0.61–0.68 μm, and XS3 (infrared) 0.79–0.89 μm) are used as classification features. The commonly used maximum likelihood classifier is used for pre-classification. The panchromatic image (0.51–0.73 μm, as shown in Fig. 3(b)) of SPOT is used for offering high spatial resolution information to fuse with XS1, XS2 and XS3.

3.2 Knowledge Extraction from Pre-Classification

The classification result of the maximum likelihood classifier is conducted for the image of the geological location under study. The landcover map after classification is shown as Fig. 3(c). A confusion matrix and Kappa index [29] (as a measurement of agreement between the classified and referenced class) are used to assess the classification results. Classification accuracies of training data are shown by the confusion matrix in Table 1. The overall accuracy and Kappa are 98.67% and 97.68%, respectively. This result indicates that the maximum likelihood classifier is good enough for image classification of this case.

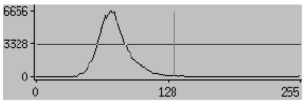

(a) histogram of total PAN image

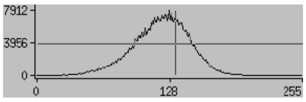

(b) histogram of PC1 of entire image

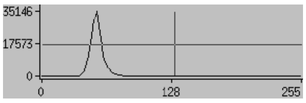

(c) histogram of class1 pixels in PAN

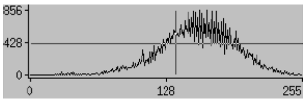

(d) histogram of PC1 of class1 pixels

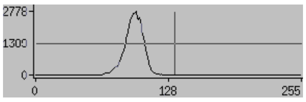

(e) histogram of class2 pixels in PAN

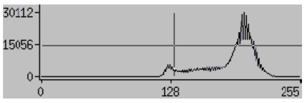

(f) histogram of PC1 of class2 pixels

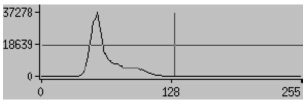

(g) histogram of class3 pixels in PAN

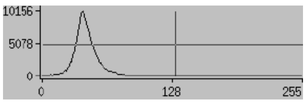

(h) histogram of PC1 of class3 pixels

Fig. 5: Histograms of PAN and PC1 (*X* axis: digital number, *Y* axis: pixel number)

3.3 Results and Discussions

From the above discussion, after pre-classification, PCA fusion not only reduces the loss of information but also relates PC1 and PAN well with their high similarities in histograms. To see the similarities, the results of principal component analysis are shown in Fig. 4, where all pixels were transfer to the PC space and Fig. 5.

When the histograms of PC1 and PAN images are of high similarity, the degree of spectral information loss is low in the replacement process [20]. Therefore, in most cases, the high resolution PAN image is linearly stretched similar (with the same mean and variance) to the to-be-replaced PC1 image before the replacement procedure.

It can be clearly seen from Fig. 5, the histogram of PC1 of the entire image is of multiple-peak distribution and the others are of single-peak distribution. Evidently, the PAN image is much easier to be stretched to the same mean and variance as the to-be-replaced images in the cases of Fig. 5(d), (f), (h) compare to the case of Fig. 5(b). On the other hand, the correlation coefficient of PAN and PC1 of the entire image 0.78 is lower than those correlation coefficients 0.89, 0.85, and 0.79 between PAN and PC1 of Class1, between PAN and PC1 of Class2, and between PC1 of Class3, respectively. From the correlation coefficient between PC1 and PAN, substantial improvements are made to the identifiable definition. The high correlation between the replaced component and the higher resolution data ensures that the spectral information of the original image is maintained. After the pre-classification procedure, principal component transform was conducted on the individual data set of each landcover class. Since the spectrum variation of each landcover class is smaller than that of the entire image, such pre-classification makes the histogram of PAN of each class more similar to the histogram of PC1, compared to that of PC1 of the entire image.

Table 2: Correlation coefficients of original and fused images

	Prior and post PCA fusion	Prior and post KBPCA fusion
XS1	0.9111	0.9208
XS2	0.8980	0.9096
XS3	0.8926	0.9839

Table 3: Information entropy of images

	Original Images	Images fused by PCA	Images fused by KBPCA
XS1	1.66	1.54	1.72
XS2	1.61	1.85	1.69
XS3	1.81	1.64	1.82
Average	1.69	1.68	1.74

Statistical assessment

Information entropy [30] and correlation coefficients of original and fused images [31] are used to assess the fusion results. The degree of the preservation of the spectral information content of a fused image can be assessed by the correlation coefficient of the original and fused images [31]. The correlation coefficients of original image and image fused by KBPCA are higher than those by PCA (see Table 2). It indicates that there is lower spectral information loss during the fusion process by KBPCA compare to that by PCA. The information entropy can be used to measure the richness of information in an image [30].

Information entropy (E) of an image can be determined with Eq. (9).

$$E = -\sum_{i=0}^{L-1} p_i \ln p_i \qquad (9)$$

where L is the number of gray levels of an image, and p_i is the ratio between the number of pixels whose gray level equals i ($0 \leqslant i \leqslant L-1$) and the total pixel number of the entire image.

The information entropies of the original image and images fused by KBPCA and PCA are shown in Table 3. The image fused by KBPCA has the largest entropy and the entropy of the image fused by PCA is larger than that of the original image. The fused images do have richer information than the original image.

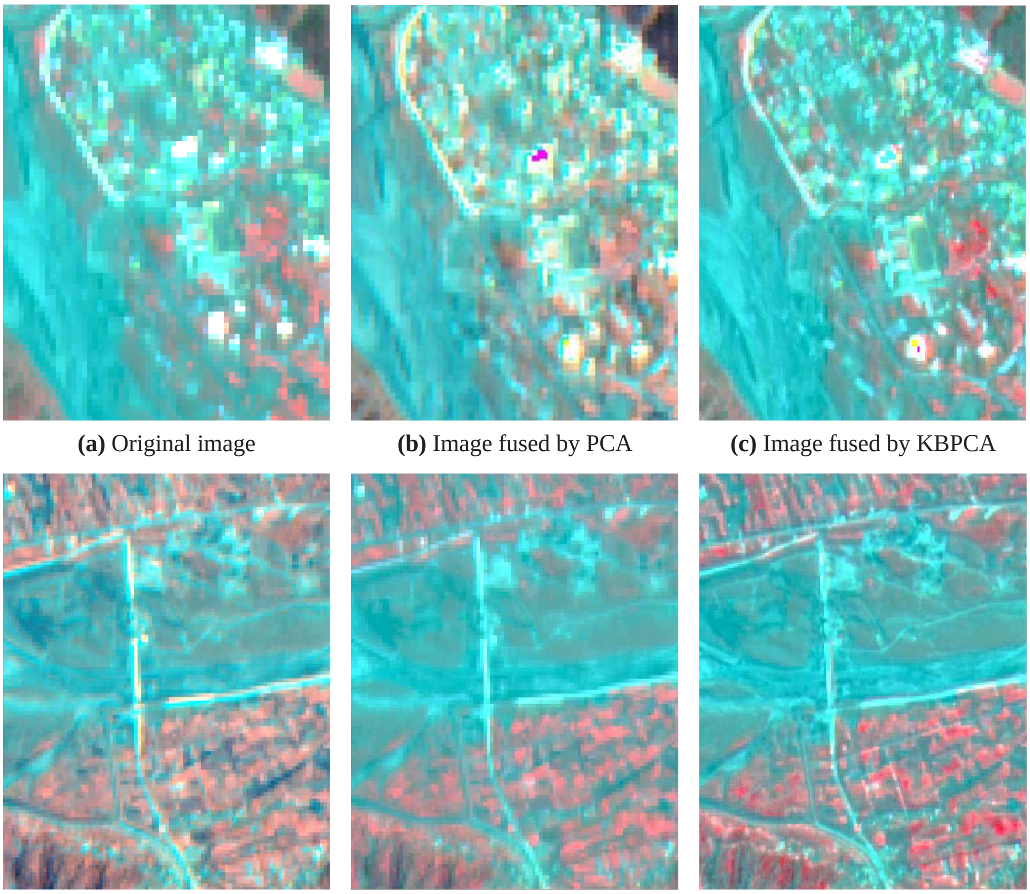

(a) Original image **(b)** Image fused by PCA **(c)** Image fused by KBPCA

(d) Original image **(e)** Image fused by PCA **(f)** Image fused by KBPCA

Fig. 6: Original images and those images fused by PCA and KBPCA

Visual assessment

The original image and fused images are shown in Fig. 6. The results of image fusion suggest that the knowledge-based PCA fusion is superior to the ordinary PCA fusion in that there are fewer color differences and clearer boundaries.

From Fig. 6, we can see that the picture in Fig. 6(c) (respectively, Fig. 6(f)) exhibits more details than that in Fig. 6(b) (respectively, Fig. 6(e)). In particular, for the pictures produced by KBPCA the boundary of urban area is more distinct and the contrast is more clear. The KBPCA result shows more details than other images. Since the knowledge-based PCA result has less distortion and color change, clearer and sharper boundary than the PCA result and that without fusion, the identifiability would be better.

4 Conclusion

A fused image contains richer in information than its original image. The main concept of the proposed KBPCA is that landcover information derived from pre-classification is used as additional information to confine spectrum variation in each class for image fusion during the principal component transformation.

The pre-classification procedure reduces the information loss in the principle component transformation and replacement process. The major information content of PC1 images is spatial information which can then be replaced by a high resolution image (PAN) with minimal information loss through the pre-classification procedure.

As a result of fusion, a multi-spectrum high resolution new image can be produced by fusing multispectral and PAN images of SPOT4. The images fused by the KBPCA method are of quality superior to those fused by the PCA method in terms of visual and statistical assessments.

The proposed KBPCA fusion can improve the fusion result of PCA approach such that the potential of application of satellite remote sensing imagery is increased. Moreover, PCA data/image fusion for other purposes may be improved by the proposed pre-classification concept as well.

Acknowledgement

Part of this research was supported by the National Science Council of Taiwan under grant NSC 100-2625-M-020-002. The authors would like to thank the National Science Council of Taiwan for financially supporting this research.

References

[1] A. Toet, J. J. V. Ruyven and J.M. Valeton, Merging thermal and visual images by a contrast pyramid, Optical Engineering, **28**, 789-792 (1989).

[2] D. M. Buede and Paul Girardi, A target identification comparison of Bayesian and Dempster-Shafer multisensor fusion, IEEE Transactions on systems, man and cybernetics-part A: systems and humans, **27**, 569-577 (1997).

[3] T. J. Hughes, Sensor fusion in a military avionics environment, Measurement and Control, **22**, 203-205 (1989).

[4] A. Toet and J. Walraven, New false colour mapping for image fusion, Optical Engineering, **35**, 650-658 (1996).

[5] H. H. Quick, H. Kuehl, G. Kaiser, D. Hornscheidt, K. P. Mikolajczyk, S. Aker, J. F. Debatin and M. E. Ladd, Interventional MRA using actively visualized catheters, trueFISP, and real-time image fusion, Magnetic Resonance in Medicine, **49**, 129-137 (2003).

[6] J. A. Nye and T. L. Faber, Current state of hybrid imaging: attenuation correction and fusion, J. Nuclear Cardiology, **18**, 729-740 (2011).

[7] C. Barillot, D. Lemoine, L. Le Briquer, F. Lachmann and B. Gibaud, Data fusion in medical imaging : merging multimodal and multipatient images identification of structures and 3D display aspects, Eur. J. Radiol, **17**, 22-27 (1993).

[8] S. E. Franklin, and C. F. Blodgett, An example of satellite multisensor data fusion, Computers and Geoscience, **19**, 577-583 (1993).

[9] B. Brisco and R. J. Brown, R. J., Multi-date SAR/VIR Synergism for Crop Classification in Western Canada, Photogrammetric Engineering and Remote Sensing, **61**, 1009-1014 (1995).

[10] Y. A. Hussin, and S. R. Shaker, Synthetic Aperture Radar, Proceedings European Conference (EUSAR '96), Berlin, Germany, 26-28 (1996).

[11] C. Son, Correlation between learning (probability of success) and fuzzy entropy in control of intelligent robot's part macro-assembly tasks with sensor fusion techniques, Robotics and Computer-Integrated Manufacturing, **23**, 47-62 (2007).

[12] Sung WT and Tsai MH, Multi-Sensor Wireless Signal Aggregation for Environmental Monitoring System via Multi-bit Data Fusion, Appl. Math. Inf. Sci., **5**, 589-603 (2011).

[13] C. Pohl, J.L. van Genderen, Multisensor image fusion in remote sensing: concepts, methods and applications, Int. J. Remote Sensing, **19**, 823-854 (1998).

[14] G. J. Briem, J. A. Benediktsson, and J. R. Sveinsson, Multiple Classifiers Applied to Multisource Remote Sensing Data, IEEE Transactions on Geoscience and Remote Sensing, **40**, 2291-2299 (2002).

[15] J. A. Malpica, Hue Adjustment to IHS Pan-Sharpened IKONOS Imagery for Vegetation Enhancement, IEEE Geoscience and Remote Sensing Letters, **4**, 27-31 (2007).

[16] Chu H and Zhu W, Fusion of IKONOS Satellite Imagery Using IHS Transform and Local Variation, IEEE Geoscience and Remote Sensing Letters, **5**, 653-657 (2008).

[17] Xue X, Zhang Q, Wei X, Guo L, and Wang Q, An Image Fusion Encryption Algorithm Based on DNA Sequence and Multi-Chaotic Maps, J. Comput. Theor. Nanosci., **7**, 397-403 (2010).

[18] Chen X, Robert Harrison, and Yan-Qing Zhang, Multi-SVM Fuzzy Classification and Fusion Method and Applications in Bioinformatics, Journal of Computational and Theoretical Nanoscience, **2**, 534–542 (2005).

[19] Schowengerdt, Remote Sensing Models and Methods for Image Processing, Robert, (1997).

[20] P. S. Chavez, S. C. Sides and J. A. Anderson, Comparison of three different method to merge multiresolution and multispectral data: Landsat TM and SPOT Panchromatic, Photogrammetric Engineering and Remote Sensing, **57**, 295-303 (1991).

[21] W. Carper, T. Lillesand and R. Kiefer, The use of intensity–hue–saturation transformation for merging SPOT panchromatic and multi-spectral image data, Photogrammetric Engineering and Remote Sensing, **56**, 459-467 (1990).

[22] G. Cliche and F. Bonn, Integration of the SPOT panchromatic channel into its multispectral mode for image sharpness enhancement, Photogrammetric Engineering and Remote Sensing, **51**, 311-316 (1985).

[23] M. González-Audícana, J. L. Saleta, R. G. Catalán and R. García., Fusion of multispectral and panchromatic images using improved IHS and PCA mergers based on wavelet decomposition, IEEE Transactions on Geoscience and Remote Sensing, **42**, 1291-1299 (2004).

[24] Sun ZL, Huang DS, Cheung YM, Liu J and Huang GB, Using FCMC, FVS, and PCA techniques for feature extraction of multispectral images, IEEE Geoscience and Remote Sensing Letters, **2**, 108-112 (2005).

[25] A. Agarwal, H. M. El-Askary, T. El-Ghazawi, M. Kafatos and J. Le-Moigne, Hierarchical PCA Techniques for Fusing Spatial and Spectral Observations With Application to MISR and Monitoring Dust Storms, IEEE Geoscience and Remote Sensing Letters, **4**, 678-682 (2007).

[26] S. Pal, T. Majumdar, and A. Bhattacharya, ERS-2 SAR and IRS-1C LISS III data fusion: A PCA approach to improve remote sensing based geological interpretation, ISPRS J. Photogrammetry and Remote Sensing, **61**, 281-297 (2007).

[27] G. Prasad, On fusion of PCA and a physical model-based predictive control strategy for efficient load-cycling operation of a thermal power plant, Optimal Control Applications and Methods, **28**, 231-258 (2007).

[28] V. P. Shah, N. H. Younan, and R. L. King, An Efficient Pan-Sharpening Method via a Combined Adaptive PCA Approach and Contourlets, IEEE Transactions on Geoscience and Remote Sensing, **46**, 1323-1335 (2008).

[29] J. L. Fleiss, Measuring nominal scale agreement among many raters, Psychological Bulletin, **76**, 378-382 (1971).

[30] Shi W, Zhu CQ, Tain Y and J. Nichol, Wavelet-based image fusion and quality assessment, Int. J. Applied Earth Observation and Geoinformation, **6**, 241-251 (2004).

[31] F. W Acerbi-Junior, J. G. P. W. Clevers, ME Schaepman, The assessment of multi-sensor image fusion using wavelet transforms for mapping the Brazilian Savanna, Int. J. Applied Earth Observation and Geoinformation, **8**, 278-288 (2006).

Jie-Lun Chiang received the M.S. degree in Dept. Agriculture engineering from National Taiwan University, Taipei, Taiwan, in 1996 and the Ph.D. degree from Dept. of Bio-environment engineering in National Taiwan University, in 2006. He is currently an Associate Professor in GIS and remote sensing with the Department of Soil and Water Conservation, National Pingtung University of Science & Technology (NPUST), Pingtung, Taiwan. His research interests include GIS, remote sensing, uncertainty of temporal-spatial data, image processing for satellite images.